

Aggregate's influence on thermophysical concrete properties at elevated temperature



Zhi Xing^{a,*}, Anne-Lise Beaucour^a, Ronan Hebert^b, Albert Noumowe^a, Béatrice Ledesert^b

^a Université de Cergy-Pontoise, L2MGC, EA 4114, F-95000 Cergy-Pontoise, France

^b Université de Cergy-Pontoise, GEC, EA 4506, F-95000 Cergy-Pontoise, France

HIGHLIGHTS

- The mineralogical nature of aggregates influences the degradation and the mass loss of concretes.
- The crystallinity degree of aggregates governs the thermal conductivity and diffusivity of concretes.
- The moisture state of concrete influenced its specific heat.
- The physical phenomena related to water appear to have a major influence on the thermal gradients of concretes.

ARTICLE INFO

Article history:

Received 27 November 2014

Received in revised form 29 April 2015

Accepted 12 July 2015

Available online 18 July 2015

Keywords:

Aggregate

Concrete

Thermal properties

High temperatures

Thermal cracking

ABSTRACT

This study investigates the thermophysical properties evolution of concretes made of three types of aggregates (quartzite, flint and limestone) during and after heating. For each aggregate type, two paste matrices ($W/C = 0.3$ and 0.6) were tested. The thermal conductivity and the specific heat are measured by a hot disk device. The evolutions of thermal properties are related to the mineral composition of aggregates but also to the microstructural evolution of concretes during heating. Evolutions of porosity, mass loss and cracking are investigated for the different concretes. The influence of aggregate's nature is then discussed regarding the thermal response of heated concrete cylinders.

© 2015 Elsevier Ltd. All rights reserved.

1. Introduction

Concrete is a composite material consisting mainly of cement paste and aggregates that is widely used in the construction of buildings and civil engineering structures. This material sometimes undergoes high temperatures in case of fire. In such event, the concrete may exhibit a thermal instability beyond a certain temperature. It results in significant degradation of concrete that compromises the safety of the structures such as tunnels of the English Channel (1996 and 2008), Mont Blanc (1999), Fréjus (2005) in France, Storebealt (1994) in Denmark, Tauern (1999) in Austria or the Gotthard tunnel (2001) in Switzerland. The fire resistance of concrete depends on the duration of fire as well as on the exposure temperature [1]. The processes of heat penetration into a concrete mass are extremely important [2]. A lesser propagation of heat causes a higher thermal gradient in the material that can increase thermal stress and therefore increase the risk of spalling.

Conversely, a poorly conducting material provides better thermal protection of steel rebars. Fourier's law can express the conduction heat transfer within the concrete by taking into account the thermal properties of concrete. The knowledge of the thermal conductivity and other thermal transport properties of concrete is essential in predicting the temperature profile and heat flow through the concrete. Indeed the heat propagation in concrete governs the chemical and structural degradation processes in a fire situation.

As aggregates occupy a large volume in concrete (around 60–80%), it is generally recognized that the heat transfer of the concrete depends mainly on the aggregates nature [3]. The mineralogical characteristics of the aggregates greatly affect the conductivity of the concrete: basalts and dolerites have a low conductivity, limestones and granites are in the middle range while quartzite and sandstone exhibit the highest conductivities [1,3,4]. The thermal conductivity of rocks commonly used as aggregates in concrete ranges from 1 to 9 W/mK [5]. At room temperature, the concretes made of aggregates containing quartz (siliceous aggregates) have a greater thermal conductivity than the concretes

* Corresponding author.

E-mail address: xzmaple@hotmail.com (Z. Xing).

made of calcareous aggregates (calcareous concrete) [3,6,7]. Moisture content and porosity of concrete also have an influence on the thermal conductivity.

Under high temperature, chemical composition, physical structure and moisture content of concrete change and the thermal properties of concrete are modified [8]. These changes are observed in the cement paste and in the aggregates and at the paste–aggregate interface [9–11]. Heating up to high temperatures causes the dehydration and decomposition of C–S–H gels (150–300 °C), Portlandite (450 °C) and calcium carbonate (700 °C) of the hardened cement paste. Aggregates also lose their evaporable water and hydrous aggregates dehydrate at high temperatures (e.g. goethite dehydrate from 250 °C), and undergo crystalline transformations accompanied by a significant volume expansion (e.g. quartz α – β transformation) [3,8]. These changes will affect the thermal properties of concretes and allow large amounts of energy consumption [12].

The thermal conductivity of concrete begins to decrease when concrete starts to lose water by evaporation and when the number of conductive connections decreases due to the decomposition of hydrates [3]. The decrease of thermal conductivity is also related to the cracking of the paste/aggregate interface, and to the disruption of the intercrystalline bonds in the aggregates due to excessive thermal expansion [10,13]. At ambient temperature, the thermal conductivity increases with the degree of crystallinity of the material (e.g. from flint to quartzite). But it decreases more with the increase of temperature for a well-crystallized structure than for a poorly-crystallized structure [14]. Moreover, according to their nature, aggregates undergo different reactions that consume heat and can change the heat transfer within the concrete. There are essentially two endothermic transformations for the aggregates: the crystalline α – β transformation of quartz (SiO_2) that occurs at 573 °C and the breakdown of calcium carbonate (CaCO_3) into free lime (CaO) and carbon dioxide (CO_2) from 600 °C [15]. These changes of aggregate properties at high temperatures influence obviously the thermal properties of concrete and therefore the heat transfer within the concrete. Physico-chemical changes occurring within the aggregates differ according to the mineral composition [11]. Therefore the choice of the aggregates is an important factor in determining the thermal properties of the concrete exposed to high temperature [16].

Few studies have compared the evolution of thermophysical properties of concretes with temperature for different types of aggregates. A comparative study of the thermal conductivity between siliceous and calcareous concrete after heating was performed by using the guarded hot plate method. The reduction of the thermal conductivity of calcareous concrete is lower than that of the siliceous aggregates with temperature [3,8]. The same phenomenon is observed in another study using a HotDisk apparatus [10]. These results are always based on residual measurements after heating–cooling cycles. The measurements of thermal conductivity of different concretes during the heating using HotDisk apparatus also showed the decrease of thermal conductivity of concrete with temperature [9,17]. The studied calcareous and silico-calcareous (flint and carbonate rock) concretes did not show many differences in thermal conductivity values because quartz in flint in the silico-calcareous aggregate is cryptocrystalline [9]. During heating, the thermal diffusivity of the concrete decreased with the increase of temperature [9,17]. No differences were pointed out between the concrete made from silico-calcareous aggregate (flints) and calcareous aggregate. According to Neville [1], the different types of aggregate have little effect on concrete specific heat. However, it is considerably increased by an increase in the moisture content. Additionally, it is known that the specific heat increases with increase in temperature and with decrease in concrete density.

The present study investigates the influence of the mineralogical nature of the aggregates on the evolution of the physical and thermal properties of concrete depending on the temperature. The thermal diffusivity and conductivity are measured during the heating up to 300 °C and then after cooling. The evolution of water–porosity and weight loss is followed after various levels of temperature up to 600 °C. The thermal conductivity being related to the evolution of porosity, these results allow to complete the analysis of the influence of the nature of the aggregates on thermal conductivity. Moreover the temperature evolution within concrete cylinders is measured by thermocouples located at their centers and surfaces. The temperature differences obtained are discussed with reference to the measurements of thermo-physical properties. Three types of aggregates are tested: calcareous, quartzite and another aggregate mostly composed of flint. For each of these aggregates, two types of concretes are studied with W/C ratios of 0.6 and 0.3. This allows comparing the relative influence of the aggregate and cementitious paste on the heat transfer.

2. Experimental program

2.1. Aggregates

Aggregates investigated in this study were crushed calcareous aggregate (C) (granular classes 6.3/14 mm and 14/20 mm), smooth rounded siliceous aggregate (S) (2/14 mm and 14/20 mm), and semi-crushed silico-calcareous aggregate (SC) (6.3/20 mm). The density of these three types of aggregate measured in the laboratory according to standard EN 1097-6 was 2670 (C), 2592 (S) and 2482 (SC) kg/m^3 with the standard deviations 0.15%, 0.11% and 0.25% respectively by five measurements. The sand used has the same composition as the aggregate and comes from the same source. Sand granular class and density are 0/4, 2686 kg/m^3 for the C aggregates that contain approximately 15% of siliceous elements, 0/2 mm, 2563 kg/m^3 for the S aggregates and 0/4 mm, 2458 kg/m^3 for the SC aggregates [11].

Using a quartering procedure [18], a representative sample of about 5 kg of each type of aggregate was obtained from an initial stock of 500 kg. The different aggregates were analyzed by macroscopic observation with a magnifying lens and using hydrochloric acid solution to react with carbonates. The different types of rocks constituting the aggregates were separated and identified at this step. Thin sections were also subsequently observed with an optical polarizing microscope to refine the classification when needed. The respective proportions of the different rock types are estimated in Table 1. The C aggregates are nearly pure carbonate, forming a homogeneous population. The S aggregates contain 91% of quartzite, about 7% of sandstone and 2% of various petrographic types. The SC aggregate presents a larger petrographic variety. It is made of flint (70%), carbonates (24%) and several other types of rock (sandstone, quartzite, etc.).

2.2. Concrete mixes

For each of the three types of aggregates, two types of concrete formulation were studied: a normal strength concrete (NSC) with a water/cement (W/C) of 0.6 and a high strength concrete (HSC) with a W/C of 0.3. Concrete compositions are listed in Table 2. Portland cement (CEMI 52.5) is used. The dosage of superplasticizer (modified polycarboxylate) is adjusted to maintain a constant workability, very plastic (S4) for all the compositions. Cylindrical specimens $\varnothing 16 \times 32$ cm are prepared. After seven days, the specimens are demoulded and placed into sealed plastic bags at ambient temperature for 90 days in agreement with the curing conditions of the RILEM recommendations [19]. Some cylindrical specimens are then cut into $\frac{1}{4} \varnothing 16 \times 5$ cm for the measurements of porosity, $\varnothing 16 \times 4$ cm for the measurements of the thermal properties of concrete during the heating or $\varnothing 16 \times 5$ cm for the study of thermal damages of concretes after heating/cooling cycles.

2.3. Equipment and set-up

The thermophysical properties of the concretes are measured during the heating in the furnace and after the exit of the furnace when the specimen is cooled. Two different furnaces were used in this study. The first is 5 l electric furnace being a part of the HotDisk device. It was used for measuring the thermal properties of the concretes with the Transient Plane Source (TPS) method. The other is an electric furnace of 1 m^3 in which $\varnothing 16 \times 32$ cm concrete cylinders were heated to investigate the evolution of concretes physical properties, visual indications of concretes degradation. The temperature evolution within concretes samples were also measured using thermocouples.

Table 1
Petrographic composition of calcareous, silico-calcareous and siliceous aggregates (values are expressed in wt.%).

Calcareous (C)		Silico-calcareous (SC)		Siliceous (S)	
Carbonate rock	99.5%	Flint	70%	Quartzite	91%
Dark Gray Carbonate	58%	Black Flint	10%	White Quartzite	28%
Dark Brown Carbonate	27%	Gray Flint	17%	Brown Quartzite	28%
Light Brown Carbonate	6.5%	Brown Flint	36%	Light Gray Quartzite	23%
Light Gray Carbonate	4%	Beige Flint	7%	Dark Gray Quartzite	10%
Red Carbonate	1%	Carbonate rock	24%	Various	2%
Multi-phase Carbonate	1.5%	White Carbonate	12%	Sandstone	7%
Calcite and carbonate rock	1.5%	Brown Carbonate	7%	Gray Sandstone	4%
Pure Calcite	Accessory	Gray Carbonate	5%	Light Sandstone	1%
Flint	Accessory	Sandstone	5%	Brown Sandstone	2%
Sandstone	Accessory	Quartzite	0.5%	Flint	1%
Iron oolite	Accessory	Micro-conglomerate	Accessory	Micro-conglomerate	Accessory
		Granite	Accessory	Shale	Accessory
		Rhyolite	Accessory	Carbonate rock	Accessory
		Basalt	Accessory	Magmatique Rock	Accessory
				Siltite	Accessory

Table 2
Mixture proportions for concrete, compressive strength, and elastic modulus of the different studied concretes.

	NSC-C	NSC-SC	NSC-S	HSC-C	HSC-SC	HSC-S
Mineralogical nature	Calcareous	Silico-calcareous	Siliceous	Calcareous	Silico-calcareous	Siliceous
Cement CEM I 52.5 (kg/m ³)	362	362	362	500	500	500
Coarse Aggregates (kg/m ³)	447	956	396	459	987	411
Fine Aggregates (kg/m ³)	625		740	646		764
Sand (kg/m ³)	714	692	585	738	715	604
Water (kg/m ³)	217	217	217	150	150	150
Superplasticizer (kg/m ³)				2.15	1.65	1.5
[% by mass of cement]				0.43%	0.33%	0.30%
W/C	0.6	0.6	0.6	0.3	0.3	0.3
Volumic Mass (kg/m ³)	2365	2227	2300	2495	2354	2431
Compressive strength (MPa) before heating	38.1	35.9	38.8	76.3	81.2	72.8
Standard deviations for compressive strengths of concrete	1.29	0.88	1.84	2.98	0.60	1.14
Tensile Strength (MPa) before heating	3.2	3.7	4	4.6	5.2	5.9
Young's Modulus (GPa) before heating	31.5	35.6	36.6	43.4	45.2	44.2

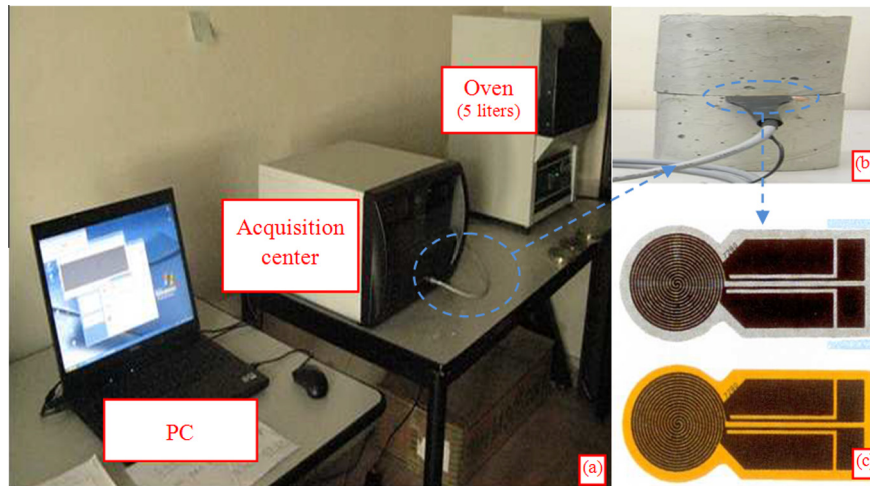


Fig. 1. Measurements of thermal properties of concretes during heating, (a) HotDisk probe TPS1500 device, (b) the placement of probe, (c) the mica probe (top) and the kapton probe (bottom).

2.3.1. Measurement of the thermal properties with TPS method

Thermal properties of concrete were measured on a pair of $\varnothing 16 \times 4$ cm cylinders with a HotDisk device. Thermal Analyser TPS1500 equipped with a high temperature furnace (Fig. 1). The system is based on the technology of the Transient Plane Source (TPS). This method has been developed at Chalmers University of Technology by Gustafsson [20]. The HotDisk sensor consists in a very fine nickel double-spiral (thickness 10 μ m) covered with two thin layers of electrically-insulating material. It is placed between two symmetrical cylinders of concrete ($\varnothing 16 \times 4$ cm) samples. The boundary surfaces of the samples were polished in order to get a plane surface and reduce the contact resistance. Specimens were pre-dried at 80 °C until constant weight before the test.

The measurements of the thermal properties of concretes were made at room temperature (20 °C), 150 °C, 225 °C and 300 °C. For the room temperature measurement, a sensor consisting of a nickel wire encased in kapton (polymer film) was used, while for the measurement performed in the furnace the nickel sensor was encased in mica (mineral). The temperature range (20–300 °C) is fixed because of the temperature limit of reuse of the mica probe. The measurements of the concrete at 150, 225 and 300 °C were performed on the same sample used at room temperature. After the cooling of the concrete specimens, their thermal properties were also measured to assess differences between thermal properties during heating and after cooling. The heating is controlled by the Analysis v5.9 software with an average rate of about 2 °C/min (Fig. 1). Before performing the thermal conductivity

measurements, it is necessary to allow a minimum of 15 h for the specimens to reach a supposed equilibrium with respect to mass (water) loss and energy redistribution through the specimen thickness, in order to get stable values with time. Three measurements are taken at one hour interval in order to prevent heat generated by the probe disturbing the thermal field of the specimen (Fig. 2).

The Hot Disc sensor acts as a constant effect generator and a resistance thermometer at the same time. During measurement, an electric current passes through the probe and creates an increase in temperature. The heat generated is dissipated through the sample on both sides at a rate that depends on the thermal transport characteristics of the material. By recording the temperature versus time response in the sensor, thermal conductivity and thermal diffusivity are determined using software provided by the manufacturer [21]. The specific heat is then determined by calculation with the density of concrete.

2.3.2. Heating–cooling cycles and temperature monitoring

The concrete specimens were subjected to different independent heating/cooling cycles with maximum temperatures fixed at 80 °C, 150 °C, 300 °C, 450 °C, 600 °C and 750 °C. Each cycle consists in three phases: a rise of temperature, stabilization at constant temperature for one hour, and then a cooling to room temperature. Heating rate is 1 °C/min and the temperature is maintained at the respective temperature for 1 h to achieve a homogeneous temperature inside the specimen. This rate is used so that the thermal gradient inside the sample will not be sufficient to create high internal stresses [10].

The heating/cooling cycles were performed in an electric furnace with size of $1.3 \times 1.1 \times 1.04$ m. The furnace allows to heat specimens up to 1000 °C. The temperature rise is controlled by a regulator-controller connected to a thermocouple in the oven. A fan associated with the heating can regulate and homogenize the temperature by air circulation between the heating elements. Thermocouples are used to monitor temperature at the upper surface and inside the concrete specimen. Type K thermocouples are connected to an automatic data acquisition system HP323 that records and transmits to the computer the temperature versus time. The surface temperature of the concrete controls the temperature rise in the oven. Type K thermocouples placed on different concrete specimens allow ensuring the temperature homogeneity in the oven.

Two thermocouples (type K.SV/SV.2 $\times 0.07$ mm²) were placed inside the test samples (Fig. 3a) to determine the temperature evolution inside the concrete specimens during the heating cycles. One thermocouple was embedded in the center of the sample during the casting of the concrete. The second one was placed on the surface of the sample before the heating cycle with a bit of mortar (Fig. 3b). The

temperature difference between the surface and the core of concrete specimens was monitored with regular intervals time during the heating–cooling cycle on cylindrical specimens ($\varnothing 16 \times 32$ cm).

2.3.3. Physical properties of concretes after heating

The water porosity of concretes was measured according to the AFREM recommendations [22]. The volume of voids is deduced from the mass difference between the dry state and the saturated surface-dry condition. The heated concrete specimens ($\frac{1}{4} \varnothing 16 \times 5$ cm) were kept in an oven at 80 °C to constant mass (M_{sc}). Once the specimens are completely dried, they are saturated and immersed for 24 h in a vacuum. They were weighed at the surface-dried state (M_{wc}) and also by hydrostatic weighing of saturated aggregates (M'_{wc}). The porosity (n) of concretes after the thermal treatment was measured with the equation $n = (M_{wc} - M_{sc}) / (M_{wc} - M'_{wc})$.

The mass difference before and after each heating–cooling cycle is investigated. Specimens are weighed immediately after the heating–cooling cycle in order to avoid a possible rehydration during the storage in ambient air. The mass loss is measured on 4 cylindrical specimens $\varnothing 16 \times 32$ cm. The mass loss percentage is obtained with equation $m_i = (m_{ai} - m_{ri}) / m_{ai} \times 100\%$, where m_i is the mass loss in %, m_{ai} is the mass of the sample at room temperature before heating and m_{ri} is the mass of the sample cooled after the heating–cooling cycle Ti.

3. Results and discussion

3.1. Influence of the nature of aggregates on concrete cracking

In order to compare and analyze the evolution of cracking with temperature in the different types of concrete, $\varnothing 16 \times 5$ cm slices were sawn from $\varnothing 16 \times 32$ cm specimens and were submitted to heating–cooling cycles at 300 °C, 600 °C and 750 °C. The highest cracking rate is observed for SC concretes using the method of surface analysis [10]. Whatever the type of aggregates used, no crack is observed after heating at 300 °C. Concretes show very different degradation forms after the heating–cooling cycle at 600 °C depending on the aggregate nature. The SC concretes show the fracture network with the longest and largest cracks. It affects

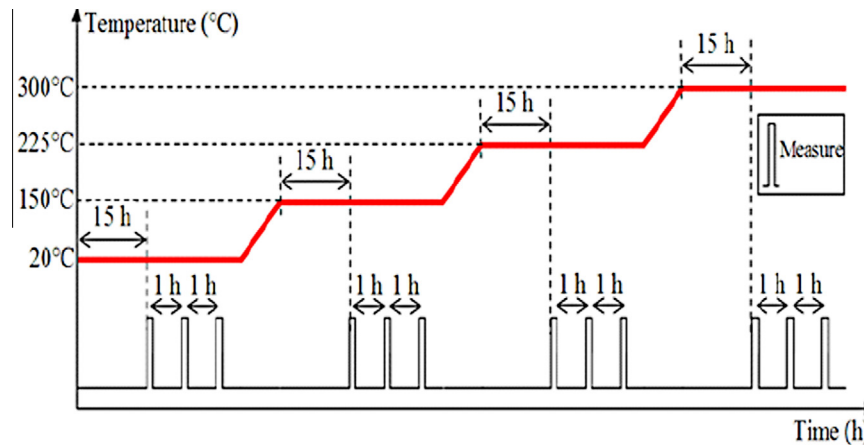


Fig. 2. Testing temperature curve for the measurement of thermal properties with TPS device.

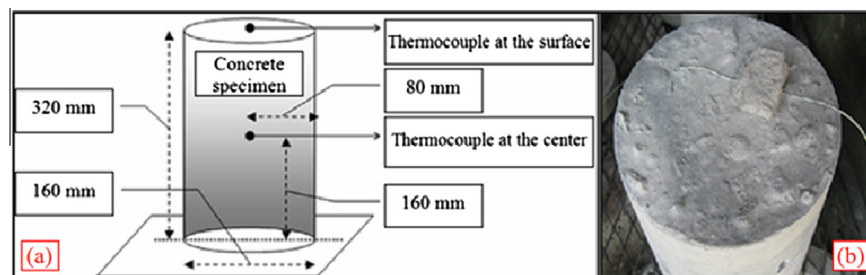


Fig. 3. Concrete specimen with thermocouples, (a) position of the thermocouples in a concrete specimen, (b) thermocouple on the concrete surface.

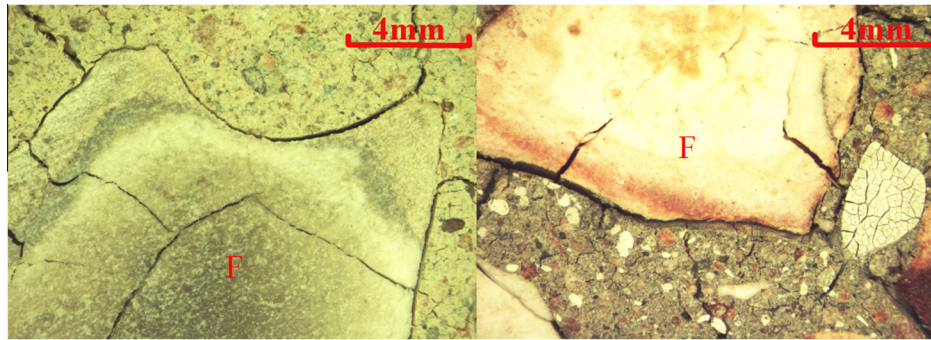


Fig. 4. Cracking of flints in NSC-SC concrete ($W/C = 0.6$) heated at 600 °C (left) and 750 °C (right). (F: flint aggregate.)

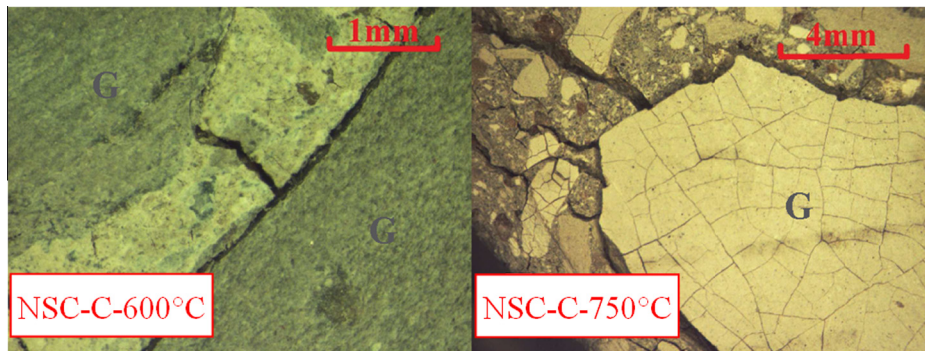


Fig. 5. Cracking of carbonates in NSC-C concrete ($W/C = 0.6$) heated at 600 °C and 750 °C. (G: carbonate aggregate.)

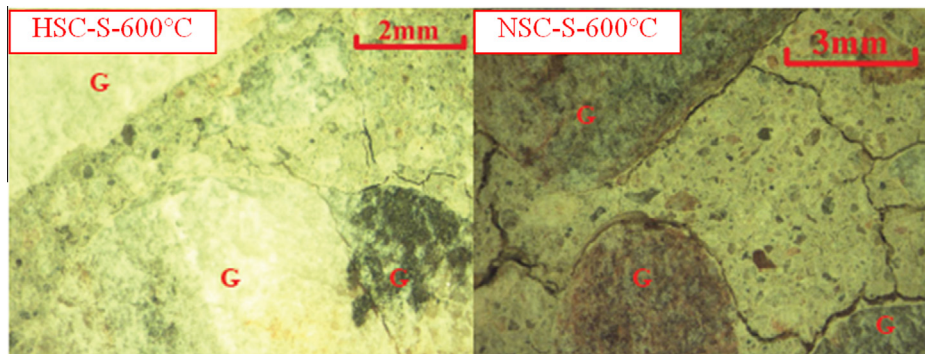


Fig. 6. Crack pattern observed in HSC-S and NSC-S at 600 °C. The transgranular crack in the left photo (quartzite is cracked), the tangential cracks at the paste/aggregate interface in the right photo (the quartzite is not damaged). (G: aggregate.)

the matrix as well as the flints that are also crossed with thin cracks (Fig. 4). The C concretes have the shortest and thinnest cracks. The S concretes are especially damaged at the periphery. Macro-cracks are sufficiently long to meet and form a connected network [10]. After the heating at 750 °C and several days of storage, concretes containing C aggregates show an additional damage. The carbonates are fragmented into small pieces (Fig. 5). This is due to the rehydration of CaO formed by the decarbonation of calcite (CaCO_3). This rehydration takes place at ambient air after the specimen exit of the furnace. This reaction between CaO and the ambient humidity leads to the formation of portlandite and a large volume expansion which causes a debonding of carbonate aggregates with the paste as well as a radial cracking. After heating at 750 °C, C aggregates are disintegrated [10]. The same phenomena are also observed for SC concretes and S concretes after the heating/cooling cycle at 750 °C, but they are much slower and less intense than in concretes with C aggregates.

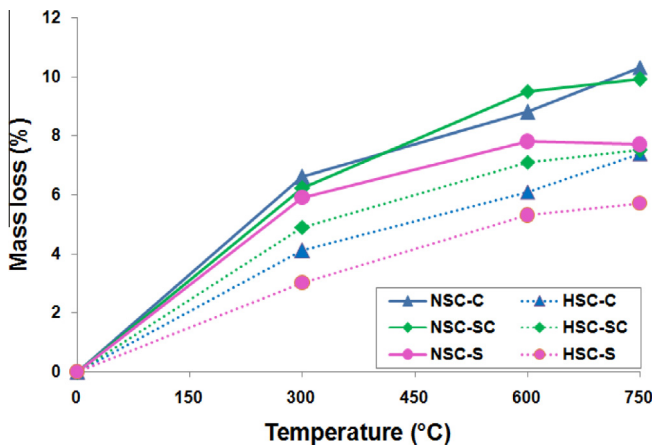
For different levels of thermal treatment, HSC appears less damaged than NSC. For the three types of aggregates, cracks in HSC have thinner openings. The difference of the cracking state between NSC and HSC is particularly remarkable in the S concrete [23]. The maximum width of cracks after heating at 600 °C is ten times smaller (30 μm instead of 300 μm) with a lower W/C ratio. Unlike the NSC, we observed the transgranular cracks in the HSC (Fig. 6) and less cracking of the paste/aggregate interface.

For the different heating temperatures, HSC concretes appear less damaged than NSC concretes. For the three types of aggregates, there is a reduction of cracks within the paste of HSC. The difference of the cracking density between normal and high strength concretes is particularly remarkable with S aggregates [23]. It can be observed under stereo microscope that the maximum width of the cracks after heating at 600 °C is ten times smaller (30 μm instead of 300 μm) for HSC-S. Unlike the NSC-S, transgranular cracks can be noticed (fracture across aggregates

Table 3

Average mass loss and standard deviation values of studied concretes after heating.

		300 °C		600 °C		750 °C	
		Average mass loss (%)	Standard deviation	Average mass loss (%)	Standard deviation	Average mass loss (%)	Standard deviation
NSC	C	6.6	0.12	8.8	0.09	10.3	0.32
	SC	6.2	0.03	9.5	0.03	9.9	0.08
	S	5.9	0.19	7.8	0.24	7.7	0.13
HSC	C	4.1	0.14	6.1	0.12	7.4	0.14
	SC	4.9	0.10	7.1	0.05	7.5	0.02
	S	3.0	0.16	5.3	0.01	5.7	0.01

**Fig. 7.** Mass loss of tested concretes as a function of the heating temperature.

and paste) in the HSC-S (Fig. 6) and less cracks following the paste-aggregate interface. This is due to the round shape and the smooth texture of the S aggregates which weakens the aggregate-bond interface strength mostly with a high W/C ratio in the concrete.

3.2. Concrete mass loss

The mass loss value is an average of the measurements carried out on 4 specimens ($\varnothing 16 \times 32$ cm) for each type of concrete. The average value and the standard deviation of mass loss for SC concretes, S concretes, and C concretes are listed in Table 3. For a given matrix (normal or high strength) the paste volume is kept unchanged for the three natures of aggregates (C, SC and S). Thus, the difference in mass loss between concretes is only related to the nature of the aggregate. For a W/C ratio of 0.6, the mass loss of the different concretes is very similar up to 300 °C. Beyond this temperature, the mineralogical composition of the aggregates influences the whole concrete mass loss (Fig. 7). For a W/C ratio of 0.3, the differences between mass losses already appear at 300 °C (Fig. 7). For HSC concretes, on the total amount of free water into the concrete, the importance of the part contained in the paste

decreases relative to the part contained in aggregates. Therefore, at 300 °C the differences in mass loss between the three HSC can be explained by the free water brought by aggregates [24]. The amounts of concrete mass loss are in accordance with the results of the mass loss of aggregates. Concretes with quartzite (S) aggregates have the lowest weight loss according to the results obtained on aggregates only [11]. The greater mass loss of SC concretes can be explained partly by the important absorbed water of the porous carbonates [9] and the departure of bound water from the flints [25]. Moreover, the mass loss of concretes with SC aggregates and with S aggregates stabilises after 600 °C. In reverse, the CO₂ gas release from calcium carbonates might explain the weight loss after 600 °C for concretes with C aggregates.

3.3. Water porosity in concretes versus temperature

Water porosity measurements provide complementary information about the thermal degradation. These measurements were carried out on 4 specimens ($\frac{1}{4} \varnothing 16 \times 5$ cm) for each type of concrete. The average value and the standard deviation of porosity for C, SC and S concretes are listed in Table 4. After heating at 80 °C, the porosity ranges from 15% to 16% for NSC and from 9% to 11% for HSC.

Fig. 8 shows the evolution of absolute and relative water porosity of concretes tested according to the heating-cooling cycles. The relative value of porosity is determined compared to the measurement made at 80 °C. Porosity increases as heating temperature rises. This increase of concrete porosity is due to the loss of adsorbed water in the capillary pores and bound water of the cement paste hydrates [6,26,27], as well as the cracking caused by differential expansion between the paste and the aggregates [6,27]. The relative increase of porosity is about 44–55% for the three types of normal strength concrete at 600 °C and about 60–75% for the high strength concretes. The relative porosity of HSC increases more strongly than that of NSC after 300 °C. However, HSC absolute porosities always remains below those of NSC. It seems that the microstructure of the more compact concrete is more affected by heating [9,28,29].

The porosity of SC concretes is always higher than that of other concretes because the porosity of carbonates in SC aggregates is twice greater than that of carbonates in C aggregates [11]. The

Table 4

Average porosity and standard deviation values of studied concretes after heating.

		80 °C		150 °C		300 °C		450 °C		600 °C	
		Average porosity (%)	Standard deviation (%)								
NSC	C	15.1	0.3	16.6	1.1	18.7	2.0	19.4	1.2	23.3	0.6
	SC	16.0	0.9	18.0	1.2	20.0	1.7	22.1	0.3	24.3	0.6
	S	15.2	0.1	16.1	2.3	18.5	2.2	19.5	2.3	21.9	0.8
HSC	C	9.9	0.2	10.2	0.8	11.5	0.3	14.1	0.7	17.2	0.4
	SC	11.3	0.3	12.4	0.5	13.0	0.4	16.9	0.2	18.3	0.4
	S	9.5	0.3	9.9	0.3	10.7	0.8	13.4	0.6	15.1	0.8

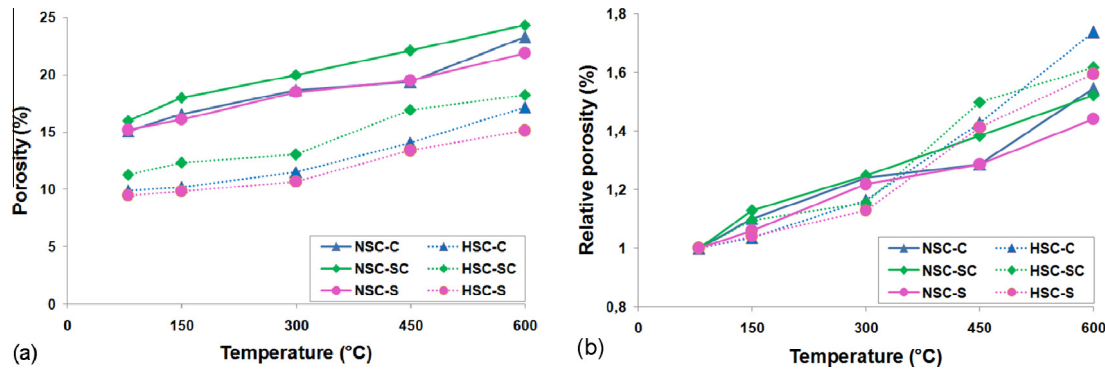


Fig. 8. Evolution of porosity for the different concretes according to the temperature, (a) absolute value; (b) relative value.

Table 5

The thermal properties average values of the studied concretes during the heating and after cooling from 300 °C.

		20 °C		150 °C		225 °C		300 °C		300 °C (after cooling)	
		Average	Standard deviation	Average	Standard deviation						
<i>Thermal conductivity λ ($W m^{-1} K^{-1}$)</i>											
NSC	C	1.63	0.110	1.55	0.024	1.42	0.006	1.34	0.001	1.54	0.13
	SC	1.86	0.080	1.76	0.001	1.59	0.004	1.46	0.007	1.78	0.10
	S	3.13	0.100	2.20	0.004	1.98	0.004	1.76	0.007	2.66	0.07
HSC	C	1.85	0.120	1.69	0.004	1.59	0.002	1.49	0.009	1.68	0.08
	SC	2.06	0.180	2.07	0.001	1.92	0.001	1.79	0.010	1.98	0.11
	S	3.33	0.140	2.84	0.022	2.50	0.002	2.19	0.007	2.88	0.17
<i>Thermal diffusivity ($mm^2 s^{-1}$)</i>											
NSC	C	0.94	0.070	0.57	0.011	0.52	0.016	0.50	0.001	0.91	0.07
	SC	1.05	0.150	0.73	0.003	0.63	0.002	0.57	0.005	1.02	0.06
	S	1.83	0.210	1.34	0.021	1.09	0.009	0.91	0.010	1.72	0.09
HSC	C	0.96	0.140	0.77	0.014	0.69	0.005	0.62	0.012	0.85	0.13
	SC	1.21	0.180	1.00	0.019	0.89	0.001	0.76	0.017	1.14	0.13
	S	1.76	0.120	1.31	0.053	1.04	0.007	0.87	0.019	1.59	0.25
<i>Volumic specific heat ($MJ m^{-3} K^{-1}$)</i>											
NSC	C	1.80	0.100	2.71	0.034	2.73	0.073	2.67	0.002	1.64	0.10
	SC	1.79	0.220	2.41	0.009	2.54	0.007	2.59	0.008	1.75	0.08
	S	1.72	0.180	1.65	0.023	1.81	0.011	1.93	0.015	1.54	0.09
HSC	C	1.94	0.270	2.18	0.034	2.31	0.013	2.40	0.033	2.01	0.24
	SC	1.72	0.110	2.08	0.039	2.15	0.004	2.37	0.030	1.75	0.11
	S	1.92	0.070	2.16	0.068	2.41	0.014	2.51	0.050	1.85	0.33
<i>Specific heat ($kJ kg^{-1} K^{-1}$)</i>											
NSC	C		0.81		1.23		1.24		1.21		0.75
	SC		0.83		1.13		1.19		1.21		0.82
	S		0.79		0.75		0.83		0.89		0.71
HSC	C		0.80		0.91		0.98		1.02		0.85
	SC		0.74		0.91		0.95		1.04		0.77
	S		0.81		0.92		1.03		1.08		0.79

comparison of the relative porosity evolution in different concretes shows that the porosity of the SC concrete increases faster between 300 °C and 450 °C than that of the other concretes. This increase in porosity at 450 °C is related to the thermal instability observed in the flints. The flints heated up to 450 °C are highly cracked. The largest increase of porosity of the SC concrete at 450 °C is the result of the thermal damage of the flints and the cracking at the paste/aggregate interface. At 450 °C, the relative porosity of quartzite (S) concretes and calcareous (C) concretes is identical. These types of aggregate are less affected for this temperature level may explain this observation. Between 450 °C and 600 °C, the porosity of C concrete has more increased than those of the S and SC concretes because of the beginning of the decarbonation of the calcareous aggregates.

3.4. Evolution of concretes thermal properties

The study of the thermal properties of concretes is essential to study the behavior of concretes at high temperature. In this section, the evolutions of the thermal conductivity, the thermal diffusivity and the specific heat of the different concretes during heating were analyzed according to the mineralogical nature of aggregates. The comparison of the concretes heated up to 300 °C and after cooling in the oven is also introduced to understand the differences in the thermal properties during heating and after cooling. Then, the temperature difference between the surface and the center of the concrete specimens allows investigating the heat distribution within the concretes according to the different natures of aggregates.

3.4.1. Thermal conductivity, thermal diffusivity and specific heat of concrete

The values of thermal conductivity, thermal diffusivity and volumic specific heat of concretes measured during the heating up to 300 °C and after cooling are presented in Table 5. The thermal conductivity and thermal diffusivity are determined simultaneously in the same measurement. These values are the result of three repeated measurements. They are performed at three temperatures 150 °C, 225 °C and 300 °C. For each temperature level, the measurement is conducted when the test sample has a uniform temperature distribution. Beyond 300 °C the mica probe cannot be reused and this is the reason why the highest tested temperature in this study was fixed at 300 °C. The samples are dried at 80 °C in an oven in order to achieve the same moisture state of the concrete before the test. The measurements at 20 °C are performed on dry samples previously dried at 80 °C. The specific heat is calculated using the concrete density presented in [23] that is measured after cooling. The dry density value of sample for the heating level of 20 °C is that of dry samples previously dried at 80 °C. The value for the heating level of 225 °C is considered equal to that measured at 300 °C.

Based on Fig. 9, at room temperature, the conductivity of the S concretes can reach 3.3 W m⁻¹ K⁻¹ instead of 1.6–2 W m⁻¹ K⁻¹ for

the other concretes. The S aggregates are composed of quartzites with a very high content of macrocrystalline quartz which has a high conductivity (6.8–12 W m⁻¹ K⁻¹ [30]) compared to that of calcite (2–3 W m⁻¹ K⁻¹ [31]). Moreover the SC aggregates contain 70% of siliceous aggregates (flints) but the thermal conductivity of the SC concretes is close to that of the C concretes. This observation is also noted by Mindeguia [9]. The difference of the thermal conductivity between the S concretes and the SC concretes is explained by the fact that the quartz in flint is cryptocrystalline and it has consequently a lower thermal conductivity than the macrocrystalline quartz in quartzite. The thermal conductivity increases with the degree of crystallinity of the material.

From 150 °C the thermal conductivities of NSC and HSC concretes decrease as temperature increases. Compared to the nature of aggregates the cement paste porosity has a lower impact on the thermal conductivity values. The conductivities of the high strength concretes are higher from 6% to 29% than those of the normal strength concretes. There is, in fact, a smaller decrease of the conductivity for C and SC concretes than for S concretes. At 300 °C, the decrease of the conductivity for S concretes is higher than 30%. The loss of thermal conductivity is related to the adsorbed water departure, the destruction of conductive bonds caused by hydrate decomposition (ettringite and CSH), and

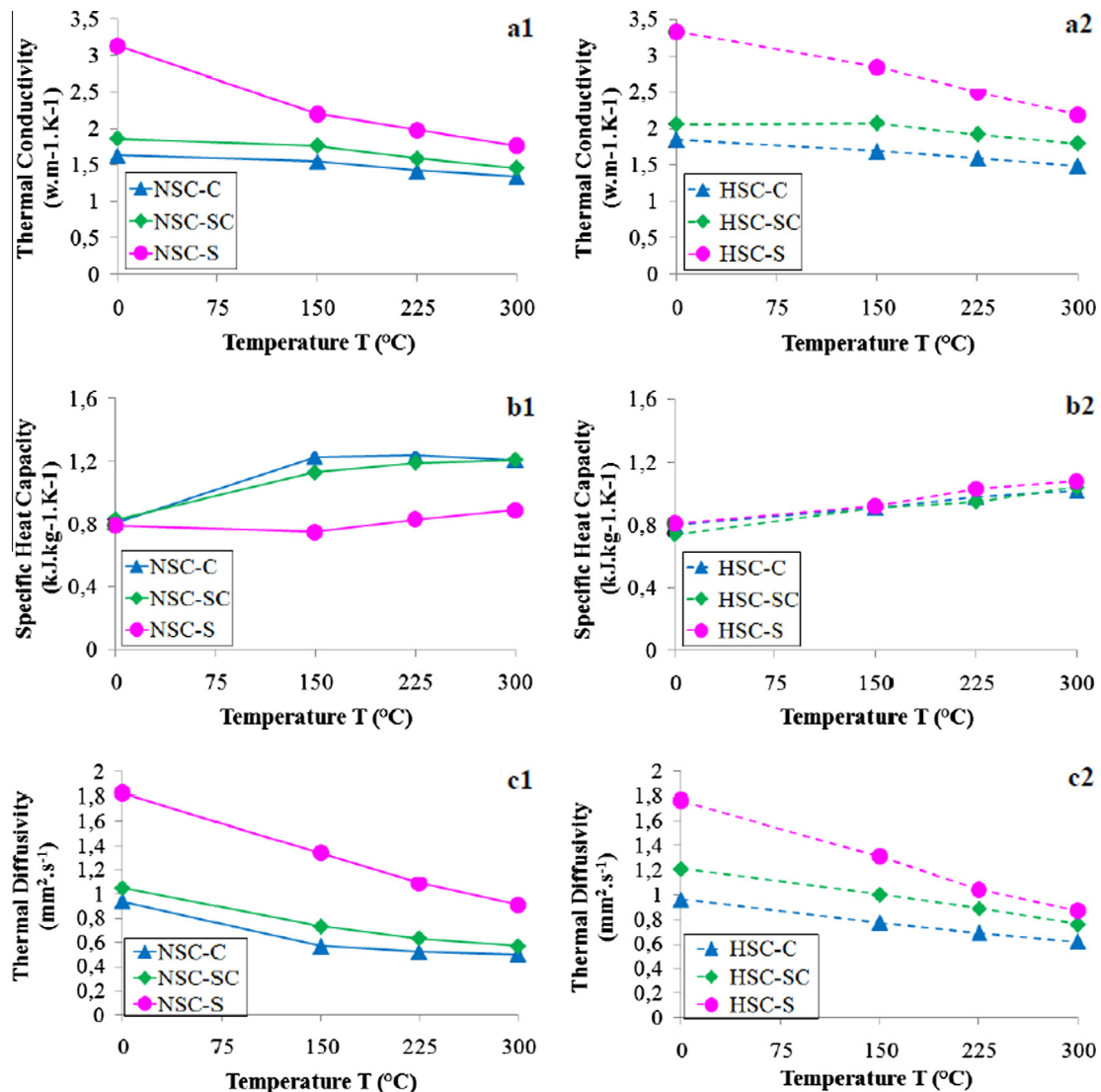


Fig. 9. The concrete thermal properties evolutions during heating (a) thermal conductivity for NSC (1) and HSC (2); (b) specific heat for NSC (1) and HSC (2); (c) thermal diffusivity for NSC (1) and HSC (2).

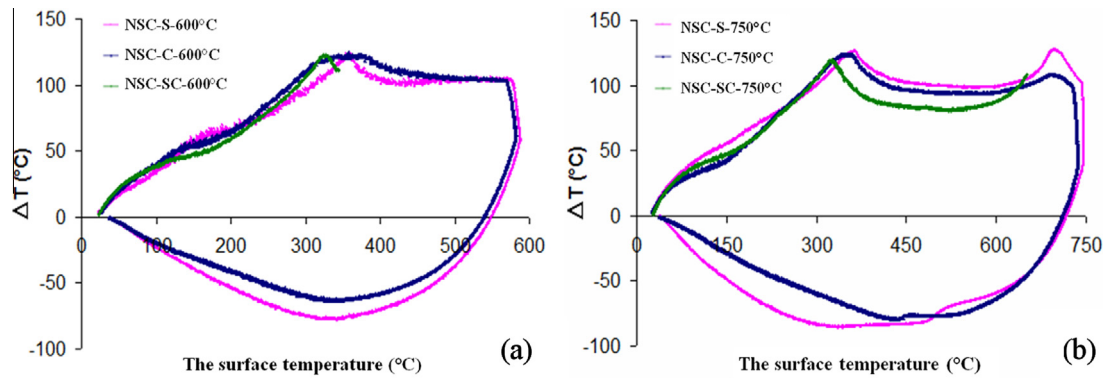


Fig. 10. Variation of temperature difference between the center and the surface of NSC-S, NSC-C and NSC-SC concretes as a function of the surface temperature for different heating-cooling cycles, (a) 600 °C; (b) 750 °C.

thermal cracking. These explanations are already identified by several researchers [3,10,11]. The higher decrease of conductivity of the S concretes cannot be explained by a higher cracking density as shown by the study of cracking and the evolution of porosity. So this difference seems inherent to the aggregates. The quartzites (91%) in the S aggregate are fully crystallized rocks, composed of macrocrystalline quartz instead of the flints where silica has a lower crystallinity degree and more defects. The thermal conductivity decreases more with the rise of temperature in well-crystallized structure than in poorly-crystallized structure [14,32].

Specimens must achieve a hydrothermal equilibrium before measurement. So it is not possible with this method to quantify the influence of the different physico-chemical transformations upon the specific heat. The specific heat measured in this study should be regarded as a fundamental specific heat, not taking into account the latent heat of different physico-chemical transformations. Fig. 9b1 and b2 shows a gentle rise of the specific heat with temperature. The specific heat of the normal strength concretes with quartzite aggregates (NSC-S) increases little compared to the concretes with calcareous aggregates (NSC-C) or silico-calcareous aggregates (NSC-SC). The concretes were previously dried in an oven at 80 °C. Theoretically, they contain almost no free water. The increase of the specific heat of NSC-C and NSC-SC, however, could be related to the presence of a small amount of water that does not evaporate during the pre-drying. The specific heat of the concretes does not depend on the nature of the aggregates, but it seems to be more influenced by the moisture state of the concrete sample. These observations are similar to those of Neville [1].

The thermal diffusivity is directly proportional to the thermal conductivity and inversely proportional to the specific heat. As the specific heat does not change a lot, the evolution of thermal diffusivity with temperature is closely linked to that of the conductivity. The thermal diffusivity of the concrete decreased with the increase of temperature. These development trends observed are similar to those of Mindeguia [9] and Jansson [17]. The thermal diffusivity of the concrete varies differently with the three types of aggregates. The thermal diffusivity of all the studied concretes decreases with the temperature rise up to 300 °C. The decrease may be explained by the departure of water, the increase of porosity and the crack formation within the material. The S concretes have a greater thermal diffusivity that decreases more greatly compared to the two other concretes (Table 5). We also do not notice an influence of the nature of the aggregate on the thermal diffusivity between the SC and the C concretes, for the reasons described above (low volume fraction of macrocrystalline quartz).

The cooling seems to have an influence on the measurement of the thermal conductivity (Table 5). Values measured after cooling

are higher than those recorded during heating. The difference is especially noticeable for NSC-S and HSC-S concretes. The works of Ödeen and Nordström [33] show also higher residual thermal conductivities than values measured during heating. But, Jansson found that the thermal conductivity remains approximately constant during the cooling after an exposure at high temperature [17]. The most important differences are observed for S concretes. It is likely that the quartz type (macrocrystalline or cryptocrystalline) in quartzite and flint aggregates plays an important role. The values measured after cooling from 300 °C are higher than those measured during heating at 300 °C for the thermal diffusivity while the specific heat values during heating are higher than those after cooling (Table 5). These differences vary from 15% to 90% compared to the values measured during heating. These differences are higher for the thermal diffusivity between the measurements during heating and after cooling [7]. The nature of aggregates also influences these differences. The differences are more important for NSC-S and HSC-S concretes.

The concrete thermal conductivity and diffusivity at ambient temperature are strongly linked to the nature of aggregates, in particular for the type of quartz (macrocrystalline or cryptocrystalline). With the rise of temperature, the influence of aggregate nature decreases. Indeed, the thermal conductivity reduction due to the temperature is marked clearly for a concrete with macrocrystalline quartz and is weaker for a calcareous aggregate concrete.

3.4.2. Thermal response

Fig. 10 shows that the temperature difference between the center and the surface of concrete specimen increases to a peak between 300 °C and 450 °C, then decreases slightly between 450 °C and 600 °C. For the 750 °C heating cycle, the temperature difference increases again and reaches the other peak between 650 °C and 700 °C. The temperature difference between the surface and the center is almost constant when comparing heating cycles up to 600 °C and 750 °C. This temperature difference is about 120–125 °C for NSC and 100–120 °C for HSC. This peak is reached at the surface temperature between 330 °C and 370 °C (first peak) and between 650 °C and 700 °C (2nd peak) for the normal strength concretes (Table 6). For the high strength concretes, the first peak occurs at slightly higher temperatures, between 335 °C and 390 °C. Conversely, the 2nd peak moves to a lower temperature. These results are similar to those found by Kanema and Pliya for the concretes made of silico-calcareous aggregates [28,34].

The temperature range where the maximum temperature differences appear corresponds to the inflection point of mass loss curve (Fig. 7). From this temperature (300 °C), the mass loss rate decreases. Most of free and bound water evaporate. However, the latent heat of vaporization delays the heat transfer from the

Table 6

The maximum temperature difference between the surface and the center of concrete specimen (ΔT), and the surface temperature (T_{surface}) corresponding to peaks for different concretes.

		Cycle 600 °C		Cycle 750 °C			
		1st peak		1st peak		2nd peak	
		ΔT (°C)	T_{surface} (°C)	ΔT (°C)	T_{surface} (°C)	ΔT (°C)	T_{surface} (°C)
NSC	C	124	358	124	355	108	693
	SC	123	328	119	327	Broken thermocouple	
	S	124	354	127	367	127	698
HSC	C	98	389	97	376	81	644
	SC	110	337	109	345	Broken thermocouple	
	S	118	366	119	370	105	669

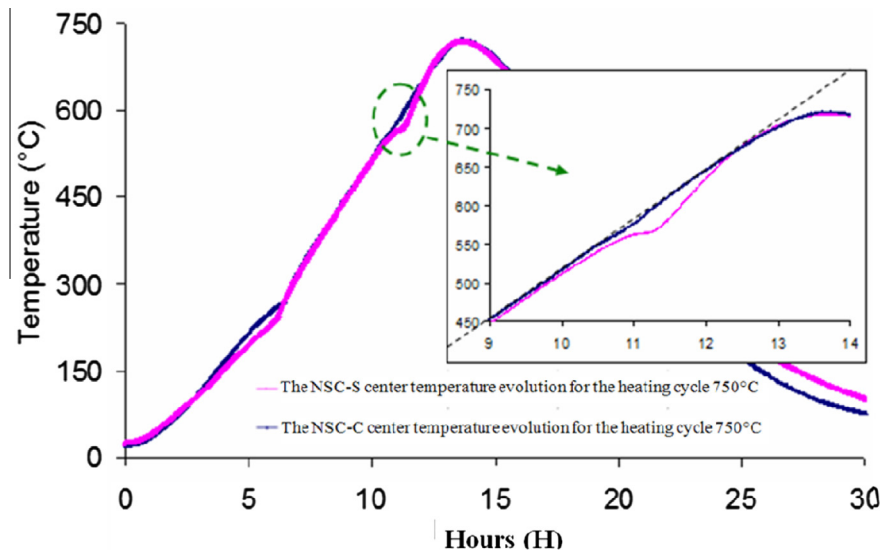


Fig. 11. The center temperature evolution for concretes with calcareous aggregates or siliceous aggregates during the heating cycle of 750 °C.

surface to the center of concrete specimen. The departure of most of the water between 100 °C and 300 °C by evaporation causes an increase in temperature difference between the surface and the center, which reaches its maximum value at about 300 °C. This temperature difference is higher for NSC (120 °C) than for HSC (110 °C) because NSC contains more free water. The surface temperatures corresponding to the first peak are lower for the NSC than for the HSC. Their higher porosity generated by a higher cracking density facilitates the migration and water departure from concrete. Similarly, NSC concretes more permeable than HSC concretes reach the first peak at lower temperature.

For NSC-SC and HSC-SC, there is a slight translation, for the first peak, to a lower surface temperature. The higher porosity in the SC concrete facilitates the transfer of water in liquid or vapor form. The maximum temperature difference occurs earlier than for the other concretes. The appearance of a second peak between 650 and 700 °C can be explained by the decomposition of portlandite in concrete [6]. The second peak is higher for the NSC-S than for the NSC-C.

The temperature evolution curve of the center of the concretes show slope change for NSC-S concrete between 550 °C and 650 °C (Fig. 11). In this temperature range, the increase of temperature within the NSC-S concrete is lower. This may be related to the allotropic transformation of quartz α to quartz β , which is slightly endothermic and occurs around 570 °C.

The higher diffusivity of NSC-S and HSC-S concretes does not influence their thermal response. The evolution of temperature within the cylindrical specimen seems more dependent on

moisture content and porosity. Water transfer and latent heat consumption seem to govern heat transfer within the concrete.

4. Conclusion

This article presents a comparative study of thermophysical properties for six concretes exposed to temperature cycles up to 750 °C analyzing the influence of the nature of aggregates. Three different types of aggregates were used as calcareous, silico-calcareous and siliceous aggregate. Two types of paste matrix were tested, normal and high strength ones. Degradation, mass loss, porosity, thermal conductivity, thermal diffusivity, specific heat and temperature difference of these concretes were studied. These properties vary depending on the aggregates types. From the results of this study, the following main conclusions can be drawn:

- The degradation of concretes made with three different types of aggregates above the heating-cooling cycle of 300 °C depends on the nature of aggregates. The SC concrete presents the highest cracking rate. The carbonates of C concrete have an additional damage as fragmentation after 750 °C. The HSC concretes show less cracking than the NSC concretes. This difference is particularly noticeable in the concrete with rounded siliceous aggregates.
- The mass loss of concretes is affected by the mineralogical nature of aggregates from the heating of 300 °C. The mass loss of C

concretes increases after 600 °C, following the departure of CO₂ from the calcite decarbonation.

- The porosity of concretes increases with the temperature. The porosity of SC concrete is always higher than that of other concretes because the carbonates in SC aggregates have porosity values twice as high as that of the carbonates of C aggregates and there is also significant cracking of SC concrete.
- The thermal conductivity and diffusivity of concretes are strongly linked to that of aggregates, in particular, the type of quartz (macrocrystalline or cryptocrystalline). For the same chemical composition of aggregates, the crystallinity degree of their minerals governs the thermal properties and its evolution with the temperature. As S concretes have ordered crystalline network, the S concretes have the higher thermal conductivity at ambient temperature. The macrocrystalline structure of quartz of quartzites aggregates can promote the stronger reduction of thermal conductivity. The cement paste compactness affects slightly the thermal conductivity values. The thermal diffusivity of concretes varies differently with the three types of aggregates in a similar trend as that of conductivity.
- The specific heat of concretes does not depend on the nature of aggregates but seems more influenced by the moisture state of concrete samples.
- The cooling seems to have little effect on the measurement of thermal conductivity for SC concrete and C concrete but greater effect on S concrete. The quartz type (macrocrystalline or cryptocrystalline) may have an important role. The values measured after cooling are higher than those measured during heating for the thermal diffusivity while the specific heat values during heating are higher than those after cooling.
- The maximum temperature difference between the surface and the center of concrete specimen does not vary with the thermal diffusivity of aggregates. Two peaks are observed and the peak appearance temperature is related to the possibility of water migration and water drainage. The first peak corresponds to the end of first phase of CSH decomposition and the second peak corresponds to the decomposition of portlandite in concrete. The physical phenomena related to water appear to have a major influence on the thermal gradients of concretes.

Acknowledgements

This work was supported by Université de Cergy-Pontoise and Laboratoire de Mécanique et Matériaux du Génie Civil in France. We thank the GSM Company for the supply of the different types of aggregate.

References

- [1] A.M. Neville, *Properties of Concrete*, fourth ed., Longman, New York, 2000.
- [2] M.A. Riley, Possible new method for the assessment of fire damaged concrete, *Mag. Concr. Res.* 43 (1991) 87–92.
- [3] Z.P. Bazant, M.F. Kaplan, *Concrete at High Temperatures*, first ed., Longman, London, 1996.
- [4] V. Kodur, W. Khaliq, Effect of temperature on thermal properties of different types of high-strength concrete, *J. Mater. Civ. Eng.* 23 (2011) 793–801.
- [5] M.I. Khan, Factors affecting the thermal properties of concrete and applicability of its prediction models, *Build. Environ.* 37 (2002) 607–614.
- [6] A. Noumowé, Effet de hautes températures (20–600 °C) sur le béton: cas particulier du béton à hautes performances, Lyon, Thèse de doctorat d'INSA de Lyon, 1995.
- [7] D.R. Flynn, Response of high performance concrete to fire conditions: review of thermal properties and measurement techniques, NIST GCR, 1999.
- [8] A.B. Kizilkanat, N. Yüzer, N. Kabay, Thermo-physical properties of concrete exposed to high temperature, *Constr. Build. Mater.* 45 (2013) 157–161.
- [9] J.C. Mindeguia, Contribution expérimentale à la compréhension des risques d'instabilité thermique des bétons, Pau: Thèse de doctorat de l'Université de Pau et des Pays de l'Adour, 2009.
- [10] Z. Xing, A.L. Beaucour, R. Hébert, A. Noumowé, B. Ledéser, Influence of the nature of aggregates on the behaviour of concrete subjected to elevated temperature, *Cem. Concr. Res.* 41 (2011) 392–402.
- [11] Z. Xing, R. Hébert, A.L. Beaucour, B. Ledéser, A. Noumowé, Influence of chemical and mineralogical composition of concrete aggregates on their behaviour at elevated temperature, *Mater. Struct.* 47 (2014) 1921–1940.
- [12] M.A. Othuman, Y.C. Wang, Elevated-temperature thermal properties of lightweight foamed concrete, *Constr. Build. Mater.* 25 (2011) 705–716.
- [13] J. Lamond, J. Pielert, Significance of Tests and Properties of Concrete and Concrete-Making Material, ASTM International, West Conshohocken, 2006.
- [14] J.P. Mercier, G. Zambelli, W. Kurz, Introduction à la science des matériaux, third ed., Presses Polytechniques et Universitaires Romandes, Lausanne, 1999.
- [15] C.A. Jouenne, *Traité de céramiques et matériaux minéraux*, Septima, Paris, 1980.
- [16] G.A. Khoury, Y. Anderberg, K. Both, J. Fellingner, N.P. Hoj, C. Majorana, Fire Design of Concrete Structures—Materials, Structures and Modelling, *Fib Bulletin* 38, 2007.
- [17] R. Jansson, Measurement of concrete thermal properties at high temperatures, in: *Fib Task Group 4.3 Workshop "Fire Design of Concrete Structures: What now? What next?"*, Milan, 2004.
- [18] R. Dupain, R. Lanchon, J.C. Saint-Arroman, *Granulats, Sols, Ciments et Bétons, Caractérisation des matériaux de génie civil par les essais de laboratoire*, second ed., Casteilla, Paris, 2000.
- [19] Rilem Technical – Committees 129-MHT, Test methods for mechanical properties of concrete at high temperatures, Part 1: introduction, Part 2: stress-strain relation, Part 3: compressive strength for service and accident conditions, *Mater. Struct.* 28 (1995) 410–414.
- [20] S.E. Gustafsson, T. Log, Transient plane source (TPS) technique for measuring thermal transport properties of building materials, *Fire Mater.* 19 (1995) 43–49.
- [21] Y. He, Rapid thermal conductivity measurement with a hot disk sensor-Part 1: theoretical considerations, *Thermochim. Acta* 436 (2005) 122–129.
- [22] AFPC-AFREM, *Compte rendu des journées techniques AFPC-AFREM Durabilité des bétons*, Toulouse: Université Paul Sabatier, 1997.
- [23] Z. Xing, Influence de la nature minéralogique des granulats sur leur comportement et celui du béton à haute température, Cergy: Thèse de doctorat de l'Université de Cergy-Pontoise, 2011.
- [24] Z. Xiao, T.C. Ling, C.S. Poon, S.C. Kou, Q. Wang, R. Huang, Properties of partition wall blocks prepared with high percentages of recycled clay brick after exposure to elevated temperatures, *Constr. Build. Mater.* 49 (2013) 56–61.
- [25] J. Verstraete, Approche multi-technique et multi-échelle d'étude des propriétés structurales des matériaux hétérogènes: application à un granulat siliceux naturel, Mulhouse: Thèse de doctorat de l'Université de Mulhouse, 2005.
- [26] C. Galle, J. Sercombe, Permeability and pore structure evolution of silico-calcareous and hematite high-strength concretes submitted to high temperatures, *Mater. Struct.* 34 (2001) 619–628.
- [27] P. Kalifa, M. Tsimbrovska, Comportement des BHP à hautes températures-Etat de la question et résultats expérimentaux, *Cahier du CSTB* 3078, 1998.
- [28] P. Pliya, Contribution des fibres de polypropylène et métalliques à l'amélioration du comportement du béton soumis à une température élevée, Cergy: Thèse de doctorat de l'Université de Cergy-Pontoise, 2010.
- [29] P. Pliya, A.L. Beaucour, A. Noumowé, Contribution of cocktail of polypropylene and steel fibres in improving the behaviour of high strength concrete subjected to high temperature, *Constr. Build. Mater.* 25 (2011) 1926–1934.
- [30] B. Gibert, D. Mainprice, Effect of crystal preferred orientations on the thermal diffusivity of quartz polycrystalline aggregates at high temperature, *Tectonophysics* 465 (2009) 150–163.
- [31] K.P. Furlong, R.B. Hanson, J.R. Bowers, Modeling thermal regimes, *Rev. Mineral. Geochim.* 26 (1991) 437–505.
- [32] T.Z. Harmathy, L.W. Allen, Thermal properties of selected masonry unit concretes, *J. Am. Concr. Inst.* 70 (1973) 132–142.
- [33] K. Ödeen, A. Nordström, Thermal properties for concrete at high temperatures, *Cement och Beton* (1972) 1 (in Swedish).
- [34] T.M. Kanéma, Influence des paramètres de formation sur le comportement à haute température des bétons, Cergy: Thèse de doctorat de l'Université de Cergy-Pontoise, 2007.